The Benefit of Cooperation in the Context of Massive MIMO

Stefan Dierks[1], Muhammad Bilal Amin[2], Wolfgang Zirwas[2] , Martin Haardt[3] and Berthold Panzner[2]
[1]Institute for Communications Engineering, Technische Universität München, Munich, Germany,
stefan.dierks@tum.de
[2] Nokia Solutions and Networks, Munich, Germany,
{bilal.amin.ext, wolfgang.zirwas, berthold.panzner}@nsn.com
[3] Communications Research Laboratory, Technische Universität Ilmenau, Germany,
martin.haardt@tu-ilmenau.de

***Abstract*— Currently a lot of research concentrates on future 5G networks for mobile radio systems of the next generation. Options like Massive MIMO (mMIMO), cooperation based on coordination or joint transmission, user equipment (UE) assisted interference cancellation, and ultra dense deployment of small cells are under discussion to achieve significant gains with respect to spectral efficiency. Massive MIMO, i.e., a strong over provisioning of antennas versus served users, is often claimed to solve many complex issues like inter cell interference, multi user MIMO scheduling, coverage holes and capacity limits. In this paper, the tradeoffs between a pure mMIMO implementation versus the combination with different types of cooperation are investigated for indoor local area scenarios.**

***Index Terms*— Cooperation, massive MIMO, channel estimation and prediction, JP CoMP, two stripe building, network MIMO, interference management.**

I. Introduction

It is expected that around 2020 the next generation of mobile radio systems, typically called the fifth generation or in short 5G, will succeed current 3GPP 4G networks. It will have to support a high diversity of requirements like efficient support of machine type communication, a low latency, increased spectral efficiency, extremely high peak data rates, and a high capacity. The capacity requirements are expected to lead to a densification of radio stations with lower transmit power, which are often called small cells (SC). On the physical layer one of the most promising enhancements is massive MIMO (mMIMO). For typical 3GPP outdoor scenarios spectral efficiencies of several tens of bits/s/Hz/cell might be possible, which corresponds to a gain by a factor of ten or more compared to todays 4G networks [see e.g. METIS deliverable D3.2].

Massive, compared to conventional MIMO, is often defined as a strong over provisioning of antennas, for example, compared to the number of served user equipments (UEs) or streams. Strong beamforming and directivity gains are claimed to relax many challenges known from conventional cellular radio systems like smart rank adaptive schedulers or highly sophisticated interference mitigation schemes.

Figure 1 illustrates the achievable capacity as a function of the number of simultaneously served UEs normalized by the number of antenna elements (AE). For lower values of simultaneously served UEs, where the mMIMO paradigm of strong over provisioning of AEs holds, the capacity increases almost linearly with the number of served UEs. Over provisioning means that the installed hardware will not be used most efficiently, which might be not acceptable considering the relative high cost of a radio frequency chain (digital-to-analogue converter, power amplifier, filter etc..) which is needed for each antenna element.

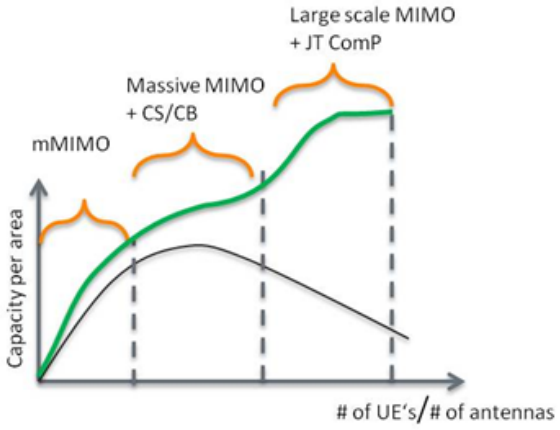

Fig. 1: Capacity versus relative number of UEs for round robin scheduled UEs (black curve) and with optimum rank selection and user grouping (green curve) including CS/CB (mid) and JT CoMP right part

A obvious idea is to add more users. Though with more and more users the multi user MIMO channel for randomly scheduled user equipments (UE) offers less degrees-of-freedom for the transmission to the UEs and interference between different cells increases. These two effects eventually outweigh the extra gain of additional users and the capacity saturates or even degrades (black curve). For medium load conditions smart rank adaptation, coordinated scheduling and coordinated beamforming (CS/CB) are known to boost performance considerably (green curve - middle).

Approaching full load conditions with similar number of UEs compared to antenna elements, joint transmission coordinated multi point (JT CoMP) can boost performance due to rank enhancement and interference mitigation.

In the end there is a trade-off between easy implementation and installation (mMIMO), and the optimal exploitation of the installed hardware (JT CoMP). Looking at the figure we can tell, that depending on the scenario JT CoMP might either increase the performance for a certain number of AEs or decrease the number of required AEs for a certain capacity target. We will investigate these trade-offs in more detail in this paper.

Massive MIMO is often seen as an outdoor technology, for example to upgrade already existing macro sites. For local area (LA) and especially indoor LA scenarios, a basic idea is to install a high number of low cost small cells (SC), ideally in almost every room. The rationale is that typically more than 70% of the mobile users are located inside buildings and indoor SCs avoid the outdoor-to-indoor penetration loss of usually more than 20 dB. In addition, short radio links of a few to tens of meters experience extremely low pathloss values.

Placing a single mMIMO array somewhere at the center of a building is not an optimal choice as users will suffer from larger transmitter-to-receiver distances together with a potentially high wall penetration loss. At the same time there is the advantage of reduced infrastructure costs when connecting a single radio site only, which motivates us to evaluate the potential of this option.

In this contribution we evaluate and verify the above mentioned trade-offs as well as the effects and the potential of massive and network MIMO (i.e., JT CoMP) for classical dual stripe office buildings. In a further step we evaluate the time variance of the LA radio channel due to moving persons and the performance of classical Kalman based channel prediction.

The scenario and system concept are described in Section II. Section III details the used transmission schemes and Section IV introduces LA performance results with no estimation error. Section V explains the channel prediction concept and Section VI assesses the effect of estimation or prediction error on massive and network MIMO. Section VII concludes the paper.

II. System Model

Consider a two stripe building defined as the A1 indoor office scenario in the WINNER II deliverable [1]. The two stripe scenario is an office building with two parallel corridors. On both sides of each corridor are rows of 10 office rooms. One office room has a size of 10m $times$ 10m, while the width of a corridor is 5m. This leads to an overall size of the building of 50m times 100m.

Two different base station deployments are considered. The first consists of a single base station at the center of the building. The second consists of four base stations (BS), where two are placed in each corridor spaced 60m apart. We denote the deployment with a single base station in the center as "Massive MIMO" and the distributed deployment as "Network MIMO".

Since we consider single antenna UEs and orthogonal frequency-division multiplexing (OFDM), we obtain independent MISO broadcast channels for each subcarrier. The received signal for one subcarrier of the k-th UE is

$$y_k = \mathbf{h}_k^H \mathbf{x} + z_k, \qquad k = 1, \ldots, K, \tag{1}$$

where $\mathbf{h}_k$ is the length M channel coefficients vector from the transmit antennas to the k-th UE and $\mathbf{x}$ is the length M transmitted signal vector. z_k is proper complex thermal Gaussian noise with variance σ_N^2, which is independent of the noise at other UEs and other subcarriers. $\mathbf{h}^H$ is the complex conjugate transpose of vector $\mathbf{h}$, respectively $\mathbf{H}^H$ of matrix $\mathbf{H}$. For more than one base station we stack the channel coefficient vectors to obtain $\mathbf{h}_k$. The total number of transmit antennas M is the sum of the number of transmit antennas at the BSs $M = \sum_i M_i$. We place the transmit antennas at one base station (BS) in a rectangular array with an antenna spacing of $\lambda/2$. The number of UEs is K, which is equal to the number of receive antennas as we consider single antenna UEs. The received signals of all UEs for one subcarrier are combined into a vector

$$\mathbf{y} = \mathbf{H}\mathbf{x} + \mathbf{z}, \tag{2}$$

where $\mathbf{y} = [y_1, \ldots, y_K]$, $\mathbf{H} = [\mathbf{h}_1, \ldots, \mathbf{h}_K]^H$ and $\mathbf{z} = [z_1, \ldots, z_K]$.

The channel coefficients are generated according to the WINNER II A1 indoor channel model [1]. The channel model provides parameter sets for line-of-sight (LOS) and non line-of-sight (NLOS) conditions. For each BS and UE the number of walls between their positions are determined and the appropriate condition is selected. An additional penetration loss of 12 dB (as we assume heavy walls) for every wall beyond the first is applied. When determining the number of walls, paths along the corridors are considered as an alternative to the direct path, which might penetrate more walls. We use the QUAsi Deterministic RadIo channel GenerAtor (QuaDRiGa) [2] to generate the channels and enhance it to count the number of walls and apply the wall penetration loss.

The number of walls for the "Massive MIMO" deployment is shown in Figure 2 and for the "Network MIMO" deployment is shown in Figure 3.

For linear precoding the vector $\mathbf{x}$ is constructed as

$$\mathbf{x} = \mathbf{W}\mathbf{s}, \tag{3}$$

where $\mathbf{W} = [\mathbf{w}_1, \ldots, \mathbf{w}_K]$ is the matrix of the precoding vectors and $\mathbf{s} = [s_1, \ldots, s_K]$ is the vector of transmit symbols. The precoding vectors are normalized $\|\mathbf{w}_k\|^2 = 1, \forall k$. We distribute the total transmit power P_S equally to the UEs. Hence the transmitted power per UE is limited by P_S/K, which can be allocated on N subcarriers. The subcarriers are organized in physical resource blocks (PRB) of 12 subcarriers, where the power allocation is done on PRB level. The transmit symbols are constraint to fulfill the per UE power constraint $\sum_{i=n}^{N} \|s_{k,n}\|^2 \leq$

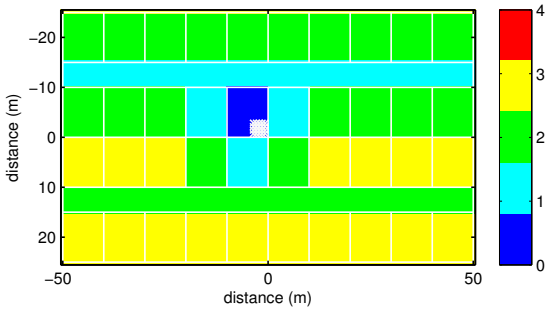

Fig. 2: Number of walls between UE position and the central BS for the "Massive MIMO" deployment

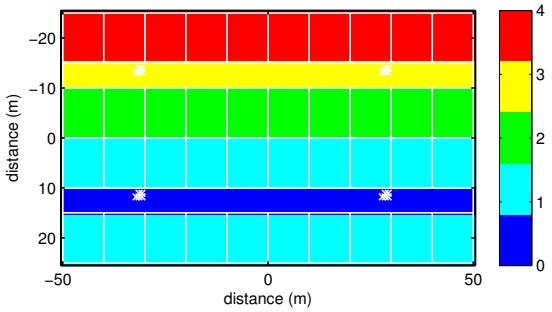

Fig. 3: Number of walls between UE position and lower right BS for the "Network MIMO" deployment

$P_S/K, \forall k$, where $s_{k,n}$ is the transmit symbol of the k-th UE on the n-th subcarrier.

III. Transmission Scheme

For the "Massive MIMO" deployment all antennas are located at one physical site, whereas for the network MIMO deployment the antennas are at different sites. To treat the distributed BSs as single BS, a sufficient backhaul connection between the BSs is needed. We assume a perfect backhaul between the BSs for the "Network MIMO" deployment. Additionally we assume a total transmit power constraint for the cooperating BSs, instead of a per BS power constraint. This way we can use the same transmission scheme for both deployments.

To determine the benefit of Network MIMO (netMIMO) versus centralized mMIMO we consider only scenarios where the total number of transmit antennas M is larger or equal to the number of UEs. Hence it is always possible to schedule all users in every time frame and on every PRB.

A. Zero Forcing Beamforming (ZFBF)

The linear precoder are determined according to an interference zero forcing objective. The optimal solution given a sum power constraint to the optimization problem is the pseudo-inverse combined with a power allocation [3]. The pseudo-inverse is

$$\mathbf{W}' = \mathbf{H}^H(\mathbf{H}\mathbf{H}^H)^{-1}. \tag{4}$$

Carrier frequency	2.1 GHz
Bandwidth	20 MHz
Used bandwidth	18 MHz
Subcarrier spacing	15 kHz
Number of subcarriers	1200
Number of PRBs	100
Antenna Spacing	$\lambda/2$
Wall penetration loss	12 dB
Sum power constraint	26 dBm
Noise level	-124.6 dBm
Maximum modulation scheme	256 QAM
Number of UEs	20
Number of drops	300
Number of channel realizations per drop	10

TABLE I: Simulation Parameters

In order to obtain a precoding matrix $\mathbf{W}$ with normalized precoders we divide the columns of $\mathbf{W}'$ by their norm

$$\mathbf{W} = \left[\frac{\mathbf{w}'_1}{\|\mathbf{w}'_1\|}, \ldots, \frac{\mathbf{w}'_K}{\|\mathbf{w}'_K\|}\right]. \tag{5}$$

With this choice of the precoding matrix the received signals become

$$\begin{aligned}\mathbf{y} &= \mathbf{H}\mathbf{W}\mathbf{s} + \mathbf{z} \\ &= \mathbf{H}\mathbf{H}^H(\mathbf{H}\mathbf{H}^H)^{-1}\mathrm{diag}\left(\frac{1}{\|\mathbf{w}'_1\|}, \ldots, \frac{1}{\|\mathbf{w}'_K\|}\right)\mathbf{s} + \mathbf{z} \\ &= \mathrm{diag}\left(\frac{1}{\|\mathbf{w}'_1\|}, \ldots, \frac{1}{\|\mathbf{w}'_K\|}\right)\mathbf{s} + \mathbf{z}. \end{aligned} \tag{6}$$

The amplitudes of the interference free channels to the UEs are the inverses of the norms of the columns of the pseudo inverse.

For a sum rate maximization with a total power constraint, the power allocation to the transmit symbols $\mathbf{s}$ can be solved using the water filling solution [3]. Here we choose to distribute the power equally to the transmission to each UE. The distribution of the per-UE power on the subcarriers is determined by the water filling solution.

IV. Simulation Results with Perfect CSI

To determine the benefit of distributed antennas with a sufficient backhaul over centralized antennas, we fix the number of UEs and compare the performance with ZFBF for different numbers of total transmit antennas. First we compare the performance of the "Massive MIMO" deployment and the "Network MIMO" deployment assuming perfect channel state information (CSI) of all links being available when determining the precoder.

We define one drop as the random placement of all 20 UEs at positions within the two stripe building. For each drop we generate 10 channel realizations. We use a bandwidth of 20 MHz around a carrier frequency of 2.1 GHz. Hence we obtain 100 PRBs, where the precoders and the power allocation are determined per PRB. The simulation parameters are summarized in Table I.

Note that we define one cell for the "Massive MIMO" deployment as the central BS and for the "Network MIMO" deployment as the cooperation cluster consisting of the four distributed BSs. Hence the maximal achievable

spectral efficiency per cell without considering control signaling overhead is

$$\frac{20 \cdot \log_2(256)\,\text{bits} \cdot 1200 \cdot 7}{0.5\,\mu s \cdot 20\,\text{MHz}} = 134.4\,\text{bit/s/Hz}, \quad (7)$$

where 20 is the number of UEs, $\log_2(256)$ are the maximal achievable bits per 256 QAM symbol, 1200 is the number of subcarriers, 7 is the number of OFDM blocks per subframe, $0.5\,\mu s$ is the duration of one subframe and 20 MHz is the bandwidth.

In Figure 4 the cumulative distribution functions (CDF) of the spectral efficiencies with ZFBF for the two deployments are shown with 20, 24, 40, 80 and 200 total transmit antennas. The solid curves correspond to the "Massive MIMO" deployment and the dashed curves to the "Network MIMO" deployment.

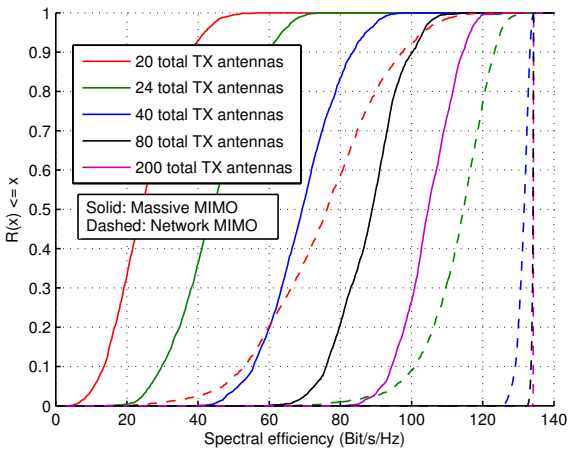

Fig. 4: CDFs of the spectral efficiencies for 20 UEs and perfect CSI

For each number of total transmit antennas the "Network MIMO" deployment clearly outperforms the "Massive MIMO" deployment. The poor performance for both deployments of the fully loaded MIMO systems with 20 transmit antennas can be improved significantly by adding only few (4) antennas. Alternatively, scheduling could be used to improve the performance for fully or close to fully loaded MIMO systems. Adding more antennas increases the performance though with decreasing gain for each additional antenna. With the "Network MIMO" deployment almost all UEs achieve the highest possible spectral efficiency for 80 total transmit antennas, while with the "Massive MIMO" deployment we do not achieve this even for 200 total transmit antennas.

A. SNR with Maximum Ratio Transmission

In this section we want to give hints to why the "Massive MIMO" deployment performs worse than the "Network MIMO" deployment. We compare the SNR achieved with maximum ratio transmission (MRT) to one UE at different positions within the two stripe building. For a system with only one UE the MRT precoder is equal to ZFBF. The performance with MRT to one UE serves as an upper bound to the performance achievable with ZFBF or any other linear precoding scheme, as serving more UEs only reduces the degrees-of-freedom. In Figures 5 and 6 the average SNR achieved with MRT are shown for the "Massive MIMO" deployment and the "Network MIMO" deployment with 20 total transmit antennas. To obtain these heat maps we average over 300 channel realizations for each sampled position.

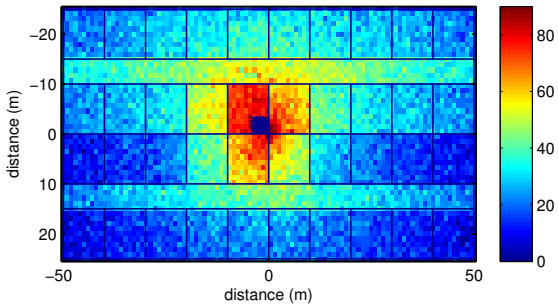

Fig. 5: Average SNR achieved with MRT to 1 UE at different positions with the "Massive MIMO" deployment and 20 total transmit antennas

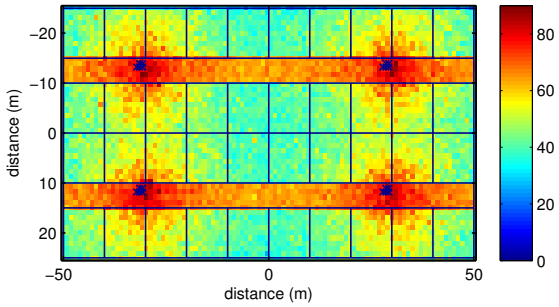

Fig. 6: Average SNR achieved with MRT to 1 UE at different positions with the "Network MIMO" deployment and 20 total transmit antennas

Note that for the "Massive MIMO" deployment in many rooms, especially those close to the outside wall, only very low SNR values are achieved. This is due to the penetration loss of the walls. Adding more antennas improves the SNR values only slightly. Whereas with the "Network MIMO" deployment the SNR values are much higher in the rooms close to the outside wall. Hence we conclude that the worse performance of the "Massive MIMO" deployment is at least partly due to the large wall penetration loss.

V. Channel Prediction on Indoor Measurements

In the previous sections, we have investigated the benefits of CoMP in the context of massive and network MIMO for local area with perfect CSI. Usually perfect CSI is not available and we have to estimate or predict the channel in some way and feedback this information. This results

in an estimation or prediction error, feedback delay and overhead which affect our overall system performance. Channel prediction can be a main enabler for network MIMO in typical 5G local area environments as it might significantly reduce the feedback overhead [5]. To assess of the typical variance of indoor radio channel conditions and to determine the benefits of channel prediction we applied state-of-the-art Kalman filtering (KF) for LA office buildings. The time-varying channel properties are derived from available indoor measurements with different degrees of user movements.

A. Kalman filter based prediction

To construct the state space model for the Kalman filter, we follow [6] and begin by modeling a single channel coefficient as an autoregressive (AR) process. This channel coefficient can either be a tap in an impulse response or the complex-valued scalar channel for a single pilot subchannel. The local scattering environment and the velocity of the UE determine the behavior of each coefficient, which is commonly oscillatory and justifies the use of AR models. The channel coefficient h_t at time t can be modeled as

$$h_t + a_1 h_{t-1} + \ldots + a_k h_{t-q} = u_t, \tag{8}$$

where q is the model order, $\{a_i\}_{i=1}^{q}$ are the AR parameters and u_t is the process noise that excites the process. The AR parameters can be estimated based on blocks of measurements. Considering we have a noise-free training segment of length N available, we can set up an over determined system of equations (Yule-Walker method)

$$\mathbf{A}\mathbf{a} = \mathbf{b}. \tag{9}$$

As an example, if we consider a time segment, $N = 100$ and a model order, $q = 4$, we may construct

$$\mathbf{A} = \begin{pmatrix} 0 & 0 & 0 & 0 \\ h_0 & 0 & 0 & 0 \\ h_1 & h_0 & 0 & 0 \\ h_2 & h_1 & h_0 & 0 \\ h_3 & h_2 & h_1 & h_0 \\ \vdots & \vdots & \vdots & \vdots \\ h_{98} & h_{97} & h_{96} & h_{95} \\ h_{99} & h_{98} & h_{97} & h_{96} \\ 0 & h_{99} & h_{98} & h_{97} \\ 0 & 0 & h_{99} & h_{98} \\ 0 & 0 & 0 & h_{99} \end{pmatrix}, \quad \mathbf{b} = - \begin{pmatrix} h_0 \\ h_1 \\ h_2 \\ h_3 \\ h_4 \\ \vdots \\ h_{99} \\ 0 \\ 0 \\ 0 \\ 0 \end{pmatrix} \tag{10}$$

A point estimate $\hat{\mathbf{a}}$ is then found by solving for $\hat{\mathbf{a}}$ in

$$(\mathbf{A}^H \mathbf{A})\hat{\mathbf{a}} = \mathbf{A}^H \mathbf{b}. \tag{11}$$

After finding $\hat{\mathbf{a}}$, we can calculate the corresponding poles $\{p_i\}_{i=1}^{q}$ of the AR process. We use these poles to construct a state space model for the fading channel coefficient h_t

$$\begin{aligned} \mathbf{x}_{t+1} &= \mathbf{X}\mathbf{x}_t + \mathbf{y}u_t, & (12) \\ h_t &= \mathbf{z}\mathbf{x}_t, & (13) \end{aligned}$$

where $\mathbf{x}_t$ is the state vector of length q. The state space is chosen on the diagonal canonical form, so that $\mathbf{X}$ is diagonal. The elements of $\mathbf{X} \in \mathcal{C}^{q\times q}$, $\mathbf{y} \in \mathcal{C}^{q\times 1}$ and $\mathbf{z} \in \mathcal{C}^{1\times q}$ are set as follows

$$\begin{aligned} \mathbf{X}[i,i] &= p_i, & (14) \\ \mathbf{y}[i] &= \prod_{\substack{j=1,\ldots,q \\ j\neq i}} (p_i - p_j)^{-1}, & (15) \\ \mathbf{z}[i] &= p_i^{q-1}, \qquad i = 1,\ldots,q & (16) \end{aligned}$$

where $\mathbf{X}[i,i]$ represents the i-th diagonal element of the matrix $\mathbf{X}$, $\mathbf{y}[i]$ and $\mathbf{z}[i]$ represent the element at index i of the vectors $\mathbf{y}$ and $\mathbf{z}$ respectively.

Now we have a state space model for just one channel coefficient. To model the complete SISO channel, we need to model each channel coefficient in the channel. We can track w parallel pilot subchannels if they are correlated. This correlation depends on the spacing between them and the coherence bandwidth of the channel. To track w subchannels, we set up a block diagonal state space

$$\begin{aligned} \mathbf{x}_{t+1}^{'} &= \text{diag}(\mathbf{X},\ldots,\mathbf{X})\mathbf{x}_t^{'} + \text{diag}(\mathbf{y},\ldots,\mathbf{y})\mathbf{u}_t, & (17) \\ &= \mathbf{A}\mathbf{x}_t^{'} + \mathbf{B}\mathbf{u}_t, & (18) \\ \mathbf{h}_t^{'} &= \text{diag}(\mathbf{z},\ldots,\mathbf{z})\mathbf{x}_t^{'} = \mathbf{C}\mathbf{x}_t^{'}, & (19) \end{aligned}$$

where $\mathbf{x}_t^{'}$ is the state vector which now has a length qw. $\mathbf{A} \in \mathcal{C}^{qw\times qw}$ is diagonal and $\mathbf{B} \in \mathcal{C}^{qw\times w}$ and $\mathbf{C} \in \mathcal{C}^{w\times qw}$ are block diagonal matrices with w blocks each. Ideally we should employ different models for individual channel coefficients, but as long as the narrowband assumption holds the same model can be used for all w subchannels.

Once we have modeled the state space, we apply the Kalman filter algorithm [6]. From the state estimate vector we can compute the channel coefficients estimate by

$$\mathbf{h}_t^{'} = \mathbf{C}\mathbf{x}_t^{'}, \tag{20}$$

and the L-step prediction estimate by

$$\mathbf{h}_{t+L}^{'} = \mathbf{C}\mathbf{A}^L\mathbf{x}_t^{'}. \tag{21}$$

B. Indoor Channel Measurements

Specific LA measurements have been performed by Umer Zeeshan in a cooperation project between NSN and TU Dresden (TUD) under the supervision of Michael Grieger. The measurements were carried out with the TUD LTE testbed within a single room of a typical office building. The BS and the UE are both static and placed at a height of 1.62 m and at a distance of 5.46 m apart from each other. The total system bandwidth is 20 MHz

and the total number of pilots 200. The carrier frequency is 2.68 GHz and the measurement is carried out for a duration of 2.1 seconds with a sampling time of 1 ms. The measurements were made for different scenarios, like the basic static case, and for cases where different number of people are moving between the BS and UE. A basic depiction of the measurement setup and the scenario where a person is moving around while waving a big board in his hand is illustrated in Figure 7

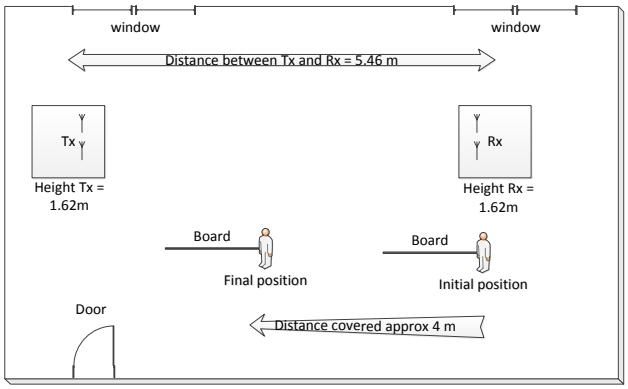

Fig. 7: A general illustration of the move-board measurement scenario

The moving people act as scatters and affect the fading behavior of the channel as can be observed in Figure 8. The channel is almost static when there is no movement between the BS and UE. When a person is moving around or additionally waving a big board (move-board scenario), we see that it induces some severe fading at select pilot subcarriers and time instances.

C. NMSE Performance of Kalman Prediction on Measurements

The time variance of the radio channel is one issue, but more interesting is how well state-of-the-art prediction like KF can exploit the relatively slow channel fluctuations. For evaluation, we track $w = 8$ parallel pilot subchannels at a time with a spacing of 90 kHz between them respecting the coherence bandwidth. As there are 200 pilot subchannels in total, we need $200/8 = 25$ parallel KFs to track the complete channel. Similarly, to ensure that the channel remains stationary during the prediction and hence the state space model remains valid, we train over a 100 ms time segment and then estimate/predict the channel for up to 100 ms. We model our channel coefficients on an AR process of order 1, as we found out that such a model represents the channels best.

We use normalized mean square error (NMSE) to characterize the performance of the predictor as it provides a direct relative measure for the degradation due to channel prediction. The NMSE is computed as an expectation over all time slots for every pilot subchannel.

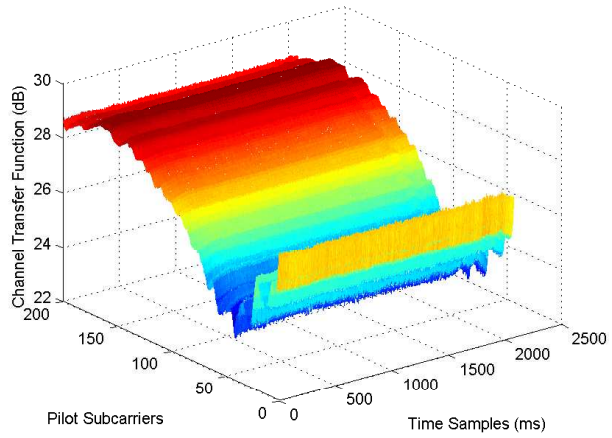

(a) Static Scenario

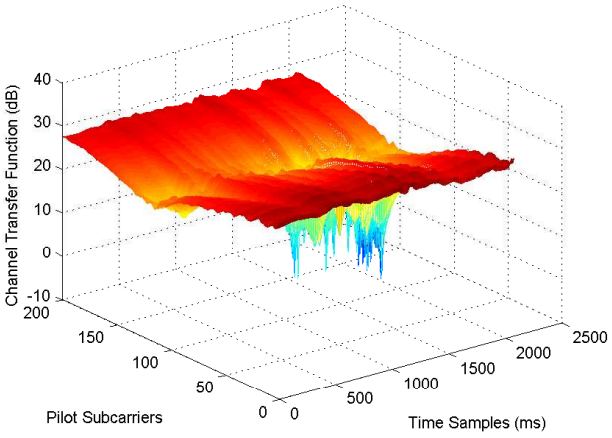

(b) One person is moving

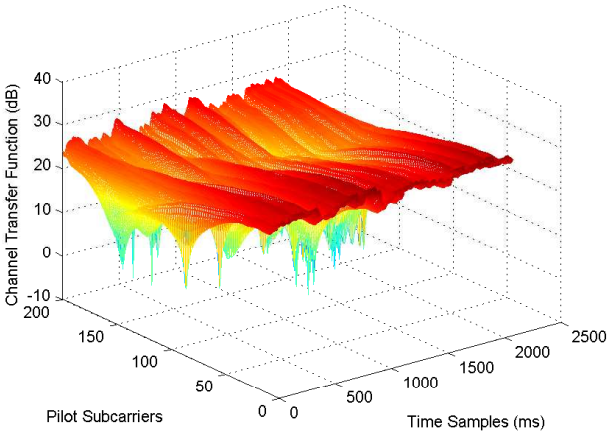

(c) A person is moving with a board

Fig. 8: The channel transfer functions (CTFs) for different measurement scenarios

$$\text{NMSE} = \sigma_E^2 = \frac{\mathrm{E}\{\|\mathbf{e}\|^2\}}{\mathrm{E}\{\|\mathbf{h}\|^2\}} = \frac{\mathrm{E}\{\|\mathbf{h} - \hat{\mathbf{h}}\|^2\}}{\mathrm{E}\{\|\mathbf{h}\|^2\}} \qquad (22)$$

Figure 9 shows NMSE performance versus prediction time for the different investigated scenarios. It was shown in [7] that an NMSE below -10 dB is required to have successful link adaptation and/or scheduling. We can see that the NMSE is below -10 dB until a prediction horizon of 28 ms for the static case and 24 ms with one person moving. This means that for LA a relative large prediction horizon with accordingly low feedback overhead seems to be possible.

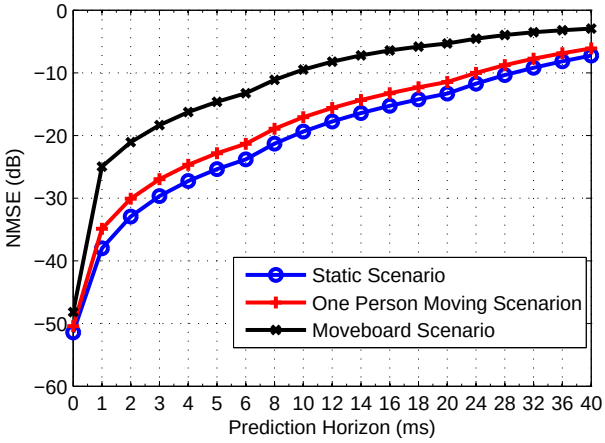

Fig. 9: NMSE performance of various scenarios at different prediction horizons

Figure 10 shows the NMSE for various time samples and pilot subchannels at a prediction horizon of 8 ms for the move-board scenario. We can observe that at most of the subchannels, the NMSE is quite similar with a mean value of -11 dB. This scenario has the worst performance out of all the three scenarios but much better prediction performance seems to be possible by proper scheduling. We can avoid to schedule users in subchannels containing frequency notches with according fast channel fluctuations, hence a higher NMSE. We see from the histogram that the error is close to Gaussian distributed.

VI. Simulation Results with Prediction Error

We analyze the effect of prediction errors on the performance of ZFBF in the two deployments. Based on the channel prediction with error $\hat{\mathbf{H}}$ the precoder are determined. When these precoder are used to transmit, interference between the UEs is introduced due to the prediction error.

In Figure 11 the spectral efficiencies for different estimation error variances achieved with 40 total transmit antennas are shown. The performances of both deployments degrade for an NMSE larger than -40 dB. The mMIMO deployment is outperformed for all NSME values clearly by the netMIMO deployment.

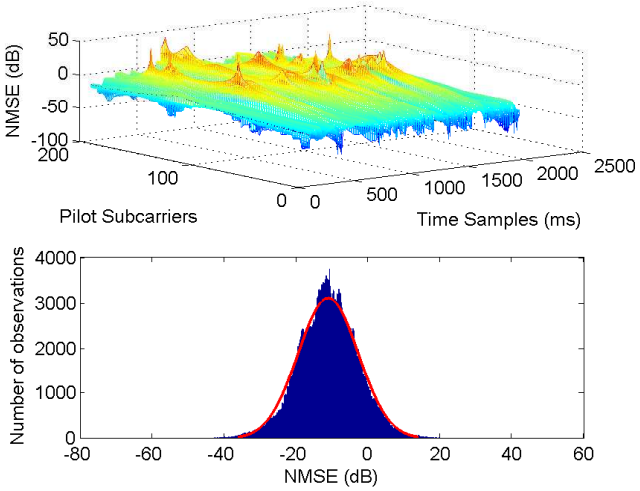

Fig. 10: NMSE at a prediction horizon of 8 ms for the move-board scenario

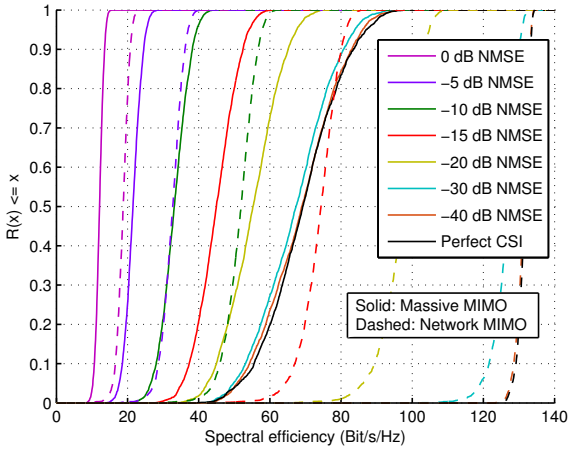

Fig. 11: CDFs of the spectral efficiencies with different estimation noise variances for 20 UEs and 40 total transmit antennas

Concluding we can state that both deployments suffer from estimation noise, while the "Network MIMO" deployment still outperforms the mMIMO deployment. More robust precoding techniques could allow a better performance in the presence of higher prediction error.

VII. Conclusions

In this work we assessed the benefits of JT CoMP, sometimes denoted as netMIMO, in the context of mMIMO and local area scenarios. With netMIMO, considerable hardware savings are possible as less antennas are needed to achieve the same spectral efficiency. With the same number of antennas significantly higher spectral efficiency is obtained. A sufficient backhaul is needed to enable netMIMO.

For a practical solution the trade-off between infrastructure costs versus costs for antenna elements, including the

radio frequency chains, should be considered. Strong over provisioning of antenna elements simplifies scheduling and decreased sensitivity to channel prediction errors for massive as well as for network MIMO systems.

For a classical Kalman based state space realization, an LA specific error model for the prediction errors was derived and used to assess the overall network and massive MIMO performance. Depending on the scenario and transmission scheme a prediction horizon of up to 28ms is achieved.

ACKNOWLEDGMENT

The research leading to these results has received funding from the European Commission's seventh framework program FP7-ICT-2009 under grant agreement n° 247223 also referred to as METIS.

S. Dierks is supported by the German Ministry of Education and Research in the framework of an Alexander von Humboldt Professorship.

We thank Michael Grieger and Umer Zeeshan for performing the indoor measurements as well as for many inspiring discussions.

REFERENCES

[1] *WINNER II Channel Models* IST-WINNER II Deliverable 1.1.2, Tech. Rep., 2008.

[2] [Online]. Available: http://www.quadriga-channel-model.de

[3] Wiesel, A.; Eldar, Y.C.; Shamai, S., *Zero-Forcing Precoding and Generalized Inverses*, IEEE Transactions on Signal Processing, vol.56, no.9, pp.4409-4418, Sept. 2008

[4] Peel, C.B.; Hochwald, B.M.; Swindlehurst, A.L., *A vector-perturbation technique for near-capacity multiantenna multiuser communication-part I: channel inversion and regularization*, IEEE Transactions on Communications, vol.53, no.1, pp.195-202, Jan. 2005

[5] Jungnickel, V.; Manolakis, K.; Zirwas, W.; Panzner, B.; Sternad, M.; Svensson, T., *The Role of Small Cells, Coordinated Multipoint and Massive MIMO in 5G*, IEEE Communications Magazine, May 2014.

[6] Aronsson, D., *Channel estimation and prediction for MIMO OFDM systems: Key design and performance aspects of Kalman-based algorithms*, Ph.D. Thesis, Uppsala University, 2011, http://www.signal.uu.se/Publications/pdf/a112.pdf.

[7] Falahati, S.; Svensson, A.; Torbjörn E.; Sternad, M., *Adaptive Modulation Systems for Predicted Wireless Channels*, IEEE Transactions on Communications, vol.52, no.2, pp.307316, Feb. 2004.